Origin of the critical temperature discontinuity in superconducting sulfur under high pressure

M. Monni,[1] F. Bernardini,[1] A. Sanna,[2] G. Profeta,[3] and S. Massidda[1]

[1]*CNR-IOM (UOS Cagliari) and Dipartimento Fisica, Università degli Studi di Cagliari, I-09042 Monserrato (CA), Italy*

[2]*Max-Planck-Institut für Mikrostrukturphysik, Weinberg 2, D-06120 Halle, Germany*

[3]*CNR-SPIN and Dipartimento di Scienze Fisiche e Chimiche, Università degli Studi dell'Aquila, Via Vetoio 10, I-67100 Coppito (L'Aquila) Italy*

(Received 16 October 2016; revised manuscript received 14 January 2017; published 28 February 2017)

Elemental sulfur shows a superconducting phase at high pressure (above 100 GPa), with critical temperatures that rise up to 20 K [Phys. Rev. B **65**, 064504 (2002); Nature (London) **525**, 73 (2015)] and presenting a jump at about 160 GPa, close to a structural phase transition to the β-Po phase. In this work we present a theoretical and fully *ab initio* characterization of sulfur based on superconducting density functional theory (SCDFT), focusing in the pressure range from 100 to 200 GPa. Calculations result in very good agreement with available experiments and point out that the origin of the critical temperature discontinuity is not related to the structural phase transition but induced by an electronic Lifshitz transition. This brings a strongly (interband) coupled electron pocket available for the superconducting condensation.

DOI: 10.1103/PhysRevB.95.064516

The extraordinary discovery of superconductivity at $\simeq$200 K in sulfur hydride at high pressure by Drodzov *et al.* [1] has revived the interest of the scientific community on electron-phonon coupling as the driving force for the superconducting condensation, able to lead to a Cooper pairing stronger than any known unconventional mechanism. It is remarkable that the prediction of a possible high-temperature superconducting phase in sulfur hydride was done by an *ab initio* investigation earlier than experimental confirmation, both in SH_2 [2] and SH_3 [3]. This is a strong indication of the predictive power of modern theoretical and computational methods in studying crystal structures, and electronic, dynamical, and superconducting properties of new materials in different thermodynamic conditions.

The experiment of Drodzov *et al.*, moreover, has demonstrated the decomposition of SH_2 under pressure and coexistence with elemental sulfur, via the reaction $3H_2S \rightarrow 2H_3S + S$ [4]. As a confirmation of this, in Ref. [1] the authors reported the superconducting critical temperature of pure sulfur as a function of pressure up to 250 GPa, finding a critical temperature as high as 20 K. This represents a relevant result on its own, considering the peculiarities of the sulfur phase diagram under high pressure.

The high-pressure superconducting properties of pure sulfur were already known. Indeed, it was considered [5] the element with the highest critical temperature, 17 K, under pressure. The high-pressure phase diagram of sulfur, like other group-IV elements, is characterized by a series of phase transitions from open and insulating structures, to more compact and metallic ones. Phase I, stable at low pressure, is formed by eight-ring structures. It transforms at 1.5 GPa in a trigonal chainlike structure (phase II). The tetragonal phase, phase III, is stable starting from 36 GPa up to 83 GPa. From 83 to 153 GPa, the structure of S is body centered monoclinic (*bcm*) with two atoms in the primitive cell [6–10]. Above 153 and up to 212 GPa [11] S presents a rhombohedral $\beta-$ Po structure (shown in Fig. 1). Superconductivity has been measured within the range of stability of the *bcm* structure [7] coexisting with a charge density wave (CDW) phase characterized by an *incommensurate* periodic modulation on the primitive structure which is present up to 135 GPa. The coexistence of the CDW phase with superconductivity is recognized as a peculiar feature of sulfur phase diagram [12] since CDW often competes with the superconducting phase. Magnetic measurements show that the superconducting transition temperature increases with pressure and abruptly jumps from 14.2 to 16.5 K at 155 ± 7 GPa [13], close to the transition from the *bcm* to the β-Po ($P \simeq 153$ GPa) [7,13]. This effect was recently confirmed by resistivity measurements under pressure performed by Drozdov *et al.* [1] even if not explicitly noted. The origin of this jump still awaits a complete explanation which we address in this work, where we revisit the superconducting phase diagram of pure sulfur by means of *ab initio* computational approach, not relying on any semiempirical parameters and investigating a wide pressure range which includes both the *bcm* and the β-Po phases.

I. METHOD

We performed first-principles density functional theory (DFT) calculations of the normal state properties of pure S under external isotropic pressure. We used the plane wave basis within the ultrasoft pseudopotential approximation [14] for the solution of the Kohn-Sham equation using the generalized gradient approximation (GGA-PBE) [15] for the exchange correlation energy. The phase diagram of S under pressure was obtained through stress minimization with the Parrinello-Rahman method. Dynamical properties and electron-phonon coupling constants were calculated by density functional perturbation theory [14,16]. The *bcm* (distorted with an incommensurate wave vector) structure (see below) was simulated adopting the β-Po phase, which represents a good approximation of the actual *bcm* structure within the pressure range studied. Indeed, the primitive cell of the β-Po structure is a subunit of the *bcm* structure, provided that the lattice parameters a_m, b_m, c_m and the angle β of the *bcm* structure satisfy the following relations: $a_m = a_r(3 + 6\cos\alpha_r)^{1/2}$, $b_m = a_r(2 - 2\cos\alpha_r)^{1/2}$, $c_m = a_r$,

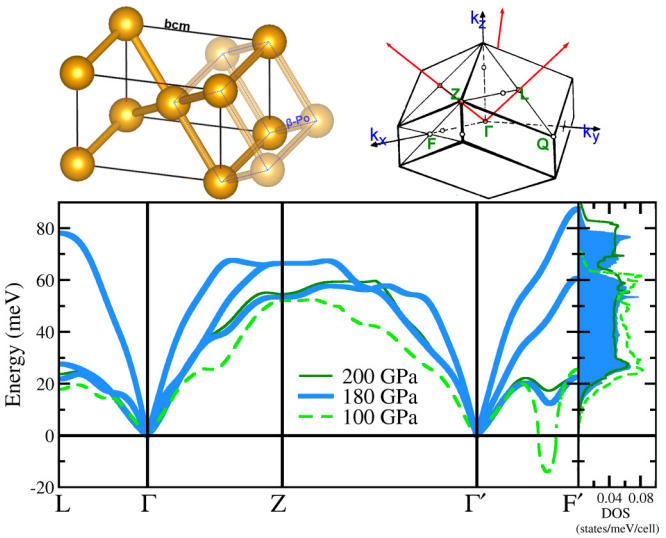

FIG. 1. (Top left) Unit cell of the *bcm* (black) and its relation with the β-Po unit cell (violet). (Top right) Brillouin zone of the rhombohedral β-Po structure. (Bottom) β-Po sulfur phonon dispersion and density of states (DOS) at 100, 180, and 200 GPa.

$\beta_m = \arccos[-(1/3 + 2/3\cos\alpha_r)^{1/2}]$, where a_r and α_r are the rhombohedral structural parameters. Therefore the *bcm* phase within the 83–153 GPa pressure range can be viewed as originating by a (slightly) symmetry-lowering deformation of the β-Po structure [12]. In our calculations we approximate the coupling of the distorted *bcm* phase with that of the β-Po phase to which we (i) remove the contribution from soft modes; (ii) scale down the density of states (DOS) at the Fermi level to simulate its reduction caused by the CDW. This reduction was computed by linear interpolation from the calculations in Ref. [12].

Calculations of superconducting properties are performed within the superconducting density functional theory (SCDFT) [17,18]. In SCDFT, we treat both electron-phonon (el-ph) and electron-electron interactions on the same ground. This avoids the consequences of treating the Coulomb interaction with the Morel-Anderson pseudopotentials μ^* [19]. The validity of the SCDFT approach was fully demonstrated in previous studies including both low- and high-pressure phases [20–29]. Recently, the method was further improved with new functionals [30] which treat the el-ph interaction in a self-consistent way. This improved version corrects a well-known tendency of the original functional to slightly underestimate the superconducting critical temperature in certain region of parameters. This last methodology was recently successfully applied in sulfur and selenium hydrides under high pressure [31], doped Black-P [32], and several other systems [33–35]. The superconducting critical temperature T_c is calculated by solving the SCDFT gap equation considering both the anisotropic wave-vector-dependent interaction as well as the multiband nature of sulfur. In addition, to highlight multiband effects, we calculated the critical temperature using two different averaging approximations for the el-ph coupling over the Fermi surface. We call the first "isotropic" because the critical temperature is obtained averaging the matrix elements over $\mathbf{k}$ space and bands. We call $T^{(\mathrm{iso})}$ the critical temperature obtained with this approach. The isotropic approximation is applied in most of the calculations based on the solution of the Eliashberg equations or using the McMillan equation to estimate T_c, because it is the computationally less expensive method to compute T_c. Although useful as a first estimation of the critical temperature, this methodology has the drawback that it does not allow to preserve the anisotropic features of the superconducting gap, which in multiband systems, MgB_2 above the others, has dramatic consequences. The second approach is named "multiband" because the average of the el-ph coupling and Coulomb screening matrix elements is performed over different groups of bands without retaining the full $\mathbf{k}$ dependence of the el-ph matrix elements. We label thereafter as $T^{(\mathrm{multi})}$ the critical temperature obtained with this approach.

The matrix elements of the Coulomb interaction screened with a static dielectric matrix, within the random phase approximation (RPA), were calculated on a mesh of $8^3 \times 8^3$ $\mathbf{k}$ and $\mathbf{k}'$ points.

II. RESULTS AND DISCUSSION

The calculated lattice constants of sulfur in the β-Po phase in the studied pressure range (β-Po phase) are in perfect agreement with previous first-principles calculations in Ref. [12].

The CDW phase is confirmed by the calculation of vibrational properties which reveal the presence of structural instability at an incommensurate wave vector. In Fig. 1, we plot the sulfur phonon dispersion along the high symmetry directions of the Brillouin zone (BZ) at 100, 180, and 200 GPa. The presence of a soft mode is evident along the Γ'-F$'$ direction at 100 GPa, underlining the presence of a modulated structure [12]. In the literature CDW instabilities are often discussed in terms of FS nesting. This point of view has been challenged by Johannes *et al.* [36] for $NbSe_2$, where no nesting was found at the CDW vector. The situation here is rather similar: At $\mathbf{q}_{\mathrm{CDW}}$ we find a peak for both the electron-phonon coupling $\lambda_{\mathbf{q},j}$ and the phonon linewidth $\gamma_{\mathbf{q},j}$, but not for the (so-called) nesting function proportional to the charge susceptibility.

Increasing the pressure, the dynamical instability disappears and we obtain positive phonon frequencies at a pressure slightly lower than 140 GPa. Thus, the experimental reported CDW phase transition, in agreement with the interpretation given in Ref. [12], can be interpreted as originating from the dynamical instability of a single phonon mode.

We point out that the presence of a structural instability related to the soft phonon mode below 140 GPa makes calculations of the superconducting coupling less reliable with decreasing pressure. This is because we are neglecting the phase transition to the distorted (uncommensurated) *bcm* structure which experimentally takes place at $P \simeq 153$ GPa [7]. However to mimic the effect of the CDW we perform the following action: (a) We cut from the calculation of the coupling the soft modes which appear for pressure below 140 GPa. Physically, this can justified considering that this mode would not contribute to the coupling due to the opening up of a CDW-type gap corresponding to their momentum transfer. (b) We (partially) consider the reduction of the electronic DOS due to the CDW distortion [12] by rescaling

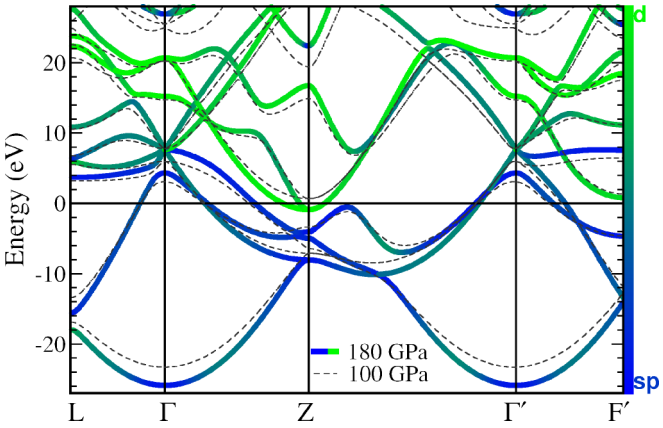

FIG. 2. Electronic band structure of sulfur in the β-Po phase at 100 (black dashed line) and 180 GPa (colored thick line). The sidebar represents the orbital character scale from blue (sp character) to green (d character)

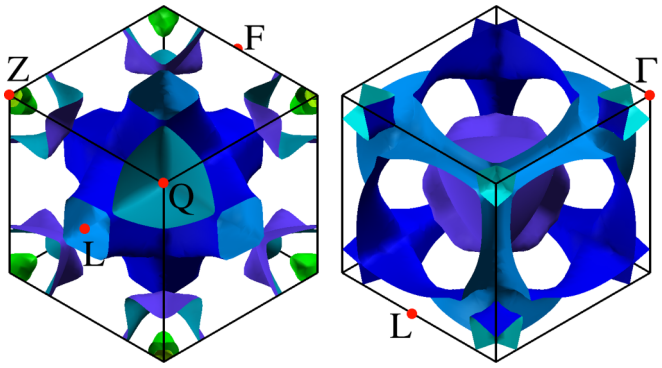

FIG. 3. Fermi surface of S in the β-Po phase at 180 GPa. The two panels show the FS centered at the Γ point (left) and centered at the Z point (right). The pockets with d character are located around the Z point.

the $\alpha^2F(\omega)$ according to calculations in Ref. [12] (as the α^2F function is proportional to the DOS [37]).

In order to understand the origin of the soft mode and the physical behavior in this pressure regime, it is interesting to examine the electronic band structure of S as a function of the pressure. In Fig. 2, we plot the energy bands for S at 100 GPa (dashed lines) and 180 GPa (thick lines), which are, respectively, below and above the CDW onset pressure (that we observe at ∼140 GPa). To highlight the orbital character of the electronic states, the bands at $P = 180$ GPa, are colored proportionally to the orbital projection (blue for sp and green for d atomic states). The low-energy (occupied) bands have a dominant sp origin, while the character changes towards d-like for the unoccupied bands above the Fermi energy. Notably, increasing pressure does not affect the band structure at the Fermi level (E_F), aside from a small widening of the valence band, indicating that the Fermi surface (FS) topology is nearly unchanged within the whole pressure range that we investigated. However, a small but remarkable exception can be found at E_F near the Z point, where two bands with a d orbital character cross E_F at $P = 180$ GPa, forming an electron pocket. We verified that this Lifshitz transition [38] happens at 130 GPa. The effect of this new band on the Fermi surface is better seen in Fig. 3, where we report the FS at $P = 180$ GPa, as seen from two different viewpoints (Γ centered in the left panel and Z centered in the right panel). The FS is composed of several extended sheets with sp character, and of two (small) d-like electron pockets around Z, whose size strongly increases with pressure above 130 GPa.

Similarly to what was discovered in potassium under pressure [22], which presents an sp-d transition in the character of band structure under pressure, we expect that more localized and directional d states can strongly couple to phonon modes. The formation of the electron pocket at the Z point may be at the origin of the disappearance of the CDW instability and the subsequent enhancement of T_c [1,13]. This hypothesis can be verified by direct calculation of the superconducting gap with the aforementioned (see Sec. I) multiband approximation. We stress that the SCDFT approach ensures that all the interactions contributing to the superconducting instability will be calculated by first principles and the behavior of T_c with pressure is only dictated by the changing on the electronic and dynamical properties of the system, without any additional parameters to fit (some) experimental data.

We solved the multiband SCDFT equations naturally grouping FS sheets as sp character sheets (FS_{sp}, first "band") and the d character sheets (FS_d, second "band"). In Fig. 4 we report the band-resolved Eliashberg functions $\alpha^2F_{ij}(\omega)$ $(i,j = sp,d)$ at $P = 180$ GPa in Fig. 4 and in Table I the relevant parameters for the two "bands" which are used in multiband SCDFT: the DOS at the Fermi level, the el-ph coupling constants (λ), and the (averaged) Coulomb matrix element (μ).

A first inspection of Table I reveals that, because of the prevalent sp character of the FS's, most of the coupling come from the intraband sp channel: $\lambda_{sp,sp} \gg \lambda_{sp,d}$.

This is highlighted by the Eliashberg functions involving sp bands, which shows a relevant coupling within all the frequency range when compared with the phonon DOS (see Fig. 4). The sheets with d character have a small intraband coupling due to the absence of small q optical phonons, which allow intraband scattering within the (small) Fermi surface. On the other hands, interband coupling with sp FS is strongly enhanced: $\lambda_{d,sp} \gg \lambda_{d,d}$. This last channel represents the most coupled (in particular for low-energy phonons) (see Fig. 4).

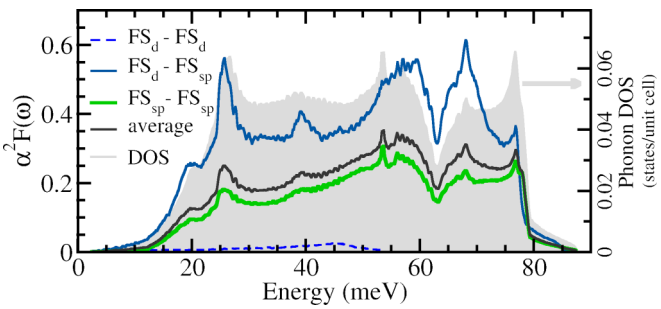

FIG. 4. Band-resolved Eliashberg functions $\alpha^2F_{ij}(\omega)$ with $i,j = sp,d$ at 180 GPa compared with the phonon density of states (filled gray curve).

TABLE I. Density of states (states/eV/spin) at the Fermi level for sp FS sheets (DOS FS_{sp}) and for d FS sheets (DOS FS_d). Electron-phonon coupling constant: mean ($\bar{\lambda}$), mediated over different FS sheets ($\lambda(FS_i - FS_j)$ with $i,j = sp,d$). Average Coulomb matrix element over the FS times the DOS at the Fermi energy (μ).

P	DOS FS_{sp}	DOS FS_d	$\bar{\lambda}$	$\lambda(FS_d - FS_d)$	$\lambda(FS_d - FS_{sp})$	$\lambda(FS_{sp} - FS_{sp})$	μ
100	0.148	0.0	0.642	0.0	0.0	0.0	0.202
120	0.142	0.0	0.630	0.0	0.0	0.0	0.192
130	0.143	0.0	0.597	0.0	0.0	0.0	0.193
140	0.138	0.0047	0.713	0.040	1.539	0.618	0.194
160	0.135	0.0086	0.742	0.055	1.421	0.604	0.194
180	0.134	0.0118	0.704	0.050	1.217	0.556	0.196
200	0.134	0.0118	0.654	0.048	1.052	0.520	0.200

We note that the band anisotropy of the el-ph is not very large: The average value of the el-ph coupling on FS $\bar{\lambda}$ (which represents the average electron-phonon coupling) is only 10% less than the maximum eigenvalue of the λ matrix, which determines T_c in the multiband BCS theory of superconductivity [39]. As a last consideration, we stress that while the el-ph coupling varies strongly with pressure, the Coulomb interaction is nearly constant over the investigated pressure range as shown in Table I.

Figure 5 reports the evolution of the calculated (full red squares) superconducting critical temperature as a function of the pressure compared with available experimental data. In the same graph, we report also the critical temperature calculated in the isotropic approximation (red circles), $T_c^{(\mathrm{iso})}$ ($T_c^{(\mathrm{multi})}$ is defined only when the d-like bands exist at the Fermi level, that is, above 130 GPa while $T_c^{(\mathrm{iso})} = T_c^{(\mathrm{multi})}$ in the case of one band). Both $T_c^{(\mathrm{multi})}(P)$ and $T_c^{(\mathrm{iso})}(P)$ show a trend in good agreement with experimental data: The sudden increase between 130 and 140 GPa is predicted with a critical temperature jump of $\simeq$6 K ($\simeq$4.5 K) for $T_C^{(\mathrm{multi})}$ ($T_C^{(\mathrm{iso})}$).

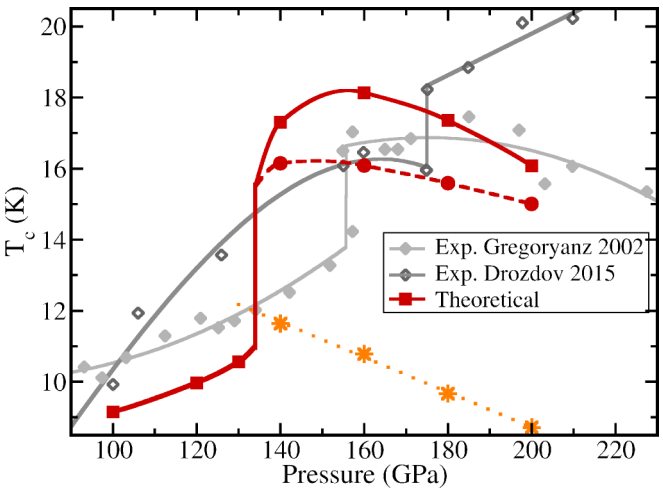

FIG. 5. Critical temperature of S as a function of pressure. (Red curves) Theoretical SCDFT calculations. A continuous line and red squares are used for the full calculation ($T_c^{(\mathrm{multi})}$); a dashed line and red points are used for $T_c^{(\mathrm{iso})}$. (Orange stars) Theoretical calculations excluding (artificially) the contribution to the phononic coupling stemming from the d electron pocket. (Full gray diamonds) Experimental data from Ref. [13]; (hollow gray diamonds) experimental data from Ref. [1]. All lines are a guide to the eyes.

For $P \leqslant 130$ GPa, the d electron pockets are empty and do not contribute to the electron-phonon coupling. For $P \geqslant 140$ GPa, $T_c^{(\mathrm{multi})}$ is always greater than $T_c^{(\mathrm{iso})}$ by 1–2 K (depending on the pressure). As shown in Table I the leading contribution to superconductivity above 140 GPa comes from the d-band coupling to sp band through to the interband channel $\lambda_{d,sp}$ giving rise to sizable off-diagonal terms of the coupling. The anisotropy of the el-ph interaction within the interband channel alone gives only a limited effect on T_c, resulting in a relatively small gain of $T_C^{(\mathrm{multi})}$ over $T_C^{(\mathrm{iso})}$.

The overall theoretical picture fits reasonably well with the existing experimental data considering the intrinsic error bar of *ab initio* methods (DFT and SCDFT functionals). In addition, we must consider that differences between the two sets of measurements exist in the critical pressure as well as in the pressure behavior (especially at high pressure). This can be surely due to the differences in the measurements (magnetic versus resistivity), to the (possible) formation of metastable phases at high pressure and in the error bar in the pressure measurement.

These results indicate that the observed jump in the critical temperature of sulfur can not be ascribed to the disappearance of a CDW phase and the corresponding effect on the DOS, but it is induced by the crossing of a new electronic band with d character and strongly coupled with phonons. This band adds a sizable contribution to the total coupling and leads to a discontinuous jump in critical temperature. This statement can be verified by a computational experiment performed artificially removing the effect of the d pocket from the coupling, that is, setting to zero all the scattering matrix elements involving this pocket. The calculated critical temperatures are significantly lower as shown in Fig. 5 (orange stars) and decreasing as a function of the pressure.

III. CONCLUSIONS

In conclusion, we have performed first-principles calculations of the electronic and dynamical properties of the high-pressure phase of sulfur reproducing the disappearance of the CDW phase at high pressure which has been considered as the main reason for the jump in the superconducting critical temperature across the transition. However, by means of extensive *ab initio* calculations of the electron-phonon coupling and superconducting critical temperature, we have shown that

another event affects the superconducting condensation: the crossing at the Fermi level of a new electronic band, with strong *d* character and significant phononic coupling. This occurrence leads to a jump in the critical temperature that compares well with the experimental evidence and that occurs at the same pressure at which the phase transition is predicted. This effect highlights the role of the Lifshitz transition in enhancing the superconducting critical temperature due to the strong coupling between phonons and directional *d* states. At the same time, we explain the origin of the high-temperature superconducting phase of sulfur, in which the disappearance of the CDW phase is concomitant with the change of the Fermi surface topology allowing new (highly) coupled scattering channels.

[1] A. P. Drozdov, M. I. Eremets, I. A. Troyan, V. Ksenofontov, and S. I. Shylin, Nature (London) **525**, 73 (2015).

[2] Y. Li, J. Hao, H. Liu, Y. Li, and Y. Ma, J. Chem. Phys. **140**, 174712 (2014).

[3] D. Duan, Y. Liu, F. Tian, D. Li, X. Huang, Z. Zhao, H. Yu, B. Liu, W. Tian, and T. Cui, Sci. Rep. **4** (2014).

[4] M. Einaga, M. Sakata, T. Ishikawa, K. Shimizu, M. I. Eremets, A. P. Drozdov, I. A. Troyan, N. Hirao, and Y. Ohishi, Nat. Phys. **12**, 835 (2016).

[5] V. V. Struzhkin, R. J. Hemley, H.-k. Mao, and Y. A. Timofeev, Nature (London) **390**, 382 (1997).

[6] O. Degtyareva, E. R. Hernndez, J. Serrano, M. Somayazulu, H.-k. Mao, E. Gregoryanz, and R. J. Hemley, J. Chem. Phys. **126**, 084503 (2007).

[7] O. Degtyareva, E. Gregoryanz, M. Somayazulu, H.-k. Mao, and R. J. Hemley, Phys. Rev. B **71**, 214104 (2005).

[8] S. P. Rudin, A. Y. Liu, J. K. Freericks, and A. Quandt, Phys. Rev. B **63**, 224107 (2001).

[9] O. Degtyareva, E. Gregoryanz, M. Somayazulu, P. Dera, H.-k. Mao, and R. J. Hemley, Nat. Mater. **4**, 152 (2005).

[10] H. Luo and A. L. Ruoff, Phys. Rev. B **48**, 569 (1993).

[11] H. Luo, R. G. Greene, and A. L. Ruoff, Phys. Rev. Lett. **71**, 2943 (1993).

[12] O. Degtyareva, M. V. Magnitskaya, J. Kohanoff, G. Profeta, S. Scandolo, M. Hanfland, M. I. McMahon, and E. Gregoryanz, Phys. Rev. Lett. **99**, 155505 (2007).

[13] E. Gregoryanz, V. V. Struzhkin, R. J. Hemley, M. I. Eremets, H.-k. Mao, and Y. A. Timofeev, Phys. Rev. B **65**, 064504 (2002).

[14] P. Giannozzi, S. Baroni, N. Bonini, M. Calandra, R. Car, C. Cavazzoni, D. Ceresoli, G. L. Chiarotti, M. Cococcioni, I. Dabo, A. Dal Corso, S. de Gironcoli, S. Fabris, G. Fratesi, R. Gebauer, U. Gerstmann, C. Gougoussis, A. Kokalj, M. Lazzeri, L. Martin-Samos, N. Marzari, F. Mauri, R. Mazzarello, S. Paolini, A. Pasquarello, L. Paulatto, C. Sbraccia, S. Scandolo, G. Sclauzero, A. P. Seitsonen, A. Smogunov, P. Umari, and R. M. Wentzcovitch, J. Phys.: Condens. Matter **21**, 395502 (2009).

[15] J. P. Perdew, K. Burke, and M. Ernzerhof, Phys. Rev. Lett. **77**, 3865 (1996).

[16] S. Baroni, P. Giannozzi, and A. Testa, Phys. Rev. Lett. **58**, 1861 (1987).

[17] M. Lüders, M. A. L. Marques, N. N. Lathiotakis, A. Floris, G. Profeta, L. Fast, A. Continenza, S. Massidda, and E. K. U. Gross, Phys. Rev. B **72**, 024545 (2005).

[18] M. A. L. Marques, M. Lüders, N. N. Lathiotakis, G. Profeta, A. Floris, L. Fast, A. Continenza, E. K. U. Gross, and S. Massidda, Phys. Rev. B **72**, 024546 (2005).

[19] P. Morel and P. W. Anderson, Phys. Rev. **125**, 1263 (1962).

[20] A. Floris, G. Profeta, N. N. Lathiotakis, M. Lüders, M. A. L. Marques, C. Franchini, E. K. U. Gross, A. Continenza, and S. Massidda, Phys. Rev. Lett. **94**, 037004 (2005).

[21] G. Profeta, C. Franchini, N. N. Lathiotakis, A. Floris, A. Sanna, M. A. L. Marques, M. Lüders, S. Massidda, E. K. U. Gross, and A. Continenza, Phys. Rev. Lett. **96**, 047003 (2006).

[22] A. Sanna, C. Franchini, A. Floris, G. Profeta, N. N. Lathiotakis, M. Lüders, M. A. L. Marques, E. K. U. Gross, A. Continenza, and S. Massidda, Phys. Rev. B **73**, 144512 (2006).

[23] A. Sanna, G. Profeta, A. Floris, A. Marini, E. K. U. Gross, and S. Massidda, Phys. Rev. B **75**, 020511 (2007).

[24] R. Akashi and R. Arita, Phys. Rev. Lett. **111**, 057006 (2013).

[25] A. Floris, A. Sanna, S. Massidda, and E. K. U. Gross, Phys. Rev. B **75**, 054508 (2007).

[26] P. Cudazzo, G. Profeta, A. Sanna, A. Floris, A. Continenza, S. Massidda, and E. K. U. Gross, Phys. Rev. Lett. **100**, 257001 (2008).

[27] R. Akashi, M. Kawamura, S. Tsuneyuki, Y. Nomura, and R. Arita, Phys. Rev. B **91**, 224513 (2015).

[28] R. Akashi and R. Arita, Phys. Rev. B **88**, 054510 (2013).

[29] R. Akashi, K. Nakamura, R. Arita, and M. Imada, Phys. Rev. B **86**, 054513 (2012).

[30] A. Sanna and E. K. U. Gross, (unpublished).

[31] J. A. Flores-Livas, A. Sanna, and E. K.U. Gross, Eur. Phys. J. B **89**, 63 (2016).

[32] A. Sanna, A. V. Fedorov, N. I. Verbitskiy, J. Fink, C. Krellner, L. Petaccia, A. Chikina, D. Y. Usachov, A. Grüneis, and G. Profeta, 2D Materials **3**, 025031 (2016).

[33] J. A. Flores-Livas and A. Sanna, Phys. Rev. B **91**, 054508 (2015).

[34] J. A. Flores-Livas, M. Amsler, C. Heil, A. Sanna, L. Boeri, G. Profeta, C. Wolverton, S. Goedecker, and E. K. U. Gross, Phys. Rev. B **93**, 020508 (2016).

[35] F. Essenberger, A. Sanna, P. Buczek, A. Ernst, L. Sandratskii, and E. K. U. Gross, Phys. Rev. B **94**, 014503 (2016).

[36] M. D. Johannes and I. I. Mazin, Phys. Rev. B **77**, 165135 (2008).

[37] The reduction is about 15% at 100 GPa and goes to zero at the β-Po to *bcm* transition that is reported to be nearly second order, involving an almost continuous distortion of the β-Po structure [7]. This approximation appears to be a good compromise between the numerical feasibility and the physical accuracy of the calculation.

[38] I. Lifshitz, ZhETF **38**, 1569 (1960) [J. Exp. Theor. Phys. **11**, 1130 (1960)].

[39] H. Suhl, B. Matthias, and L. Walker, Phys. Rev. Lett. **3**, 552 (1959).